Nordic Process Control Workshop 2012: State Estimation of a Pilot Anaerobic Digestion Reactor

Finn Haugen* Rune Bakke† Bernt Lie‡

Abstract

The Unscented Kalman Filter (UKF) with a proper state augmentation is applied to a physical anaerobic digestion (AD) reactor for estimation of physical state variables and unknown concentrations of the reactor feed. The model on which the estimator is based is a first principles mathematical model of the reactor with four state variables originally developed by D. T. Hill (1983), but modified in this study. The model is adapted to the AD reactor using data from online sensors and lab analysis. The traditional Extended Kalman Filter (EKF) is also applied to the reactor. EKF gives similar performance as the UKF, but the UKF is easier to reconfigure when the model is changed.

Keywords: State estimation; Unscented Kalman Filter; State Augmentation; Anaerobic Digestion Reactor.

1 Introduction

1.1 Background

Anaerobic digestion (AD) of animal wastes can produce biogas with methane to be used as an energy source (Tchobanoglous et al, 2003). Moreover, AD reduces methane emission, odours and contaminants. AD bioreactors are effective as they allow for relatively high load rates (feed rates) and small reactor volumes.

It is desirable to have a computer-based state estimator for an AD reactor for several reasons:

- To have estimates of non-measured state variables for the purpose of monitoring and control, possibly in a state-feedback based control system. The most important state in this respect is the (total) concentration of volatile fatty acids (VFA). High VFA concentrations are inhibitory to methane generating microbes, called methanogens, and may cause reactor instability. It is desirable if VFA concentration can be estimated continuously. An online VFA analysator is not feasible in most applications.
- To have estimates of concentrations in the reactor feed. Such estimates can be used to indicate the biogas potential of the feed.
- To have a methane gas flow estimate which is less noisy than what is obtained from raw measurements.
- To have a methane gas flow estimate in situations where biogas concentration sensors and/or biogas flow sensors have an outage.

In this study state estimators are developed for a continuous flow pilot AD reactor of 220 L, which is a part of Foss Biolab located at Foss dairy farm in Skien, Norway (a description is given in the following section). The state estimators are applied to simulated

*Telemark University College, Porsgrunn, Norway. (Tel: +47 35575000; e-mail: finn.haugen@hit.no).
†Telemark University College, Porsgrunn, Norway. (Tel: +47 35575000; e-mail: rune.bakke@hit.no)
‡Telemark University College, Porsgrunn, Norway. (Tel: +47 35575000; e-mail: bernt.lie@hit.no)

data and to measured data from the physical reactor. The estimators are ordinary and augmented Extended Kalman Filters and ditto Unscented Kalman Filters, and a simulation-estimator (or ballistic, open-loop estimator). All estimators are based on a modified version of a first principles model of the reactor with four state variables originally developed by D. T. Hill (1983). The model has been adapted to the AD reactor using data from online sensors and lab analysis.

1.2 Foss Biolab and the anaerobic digestion (AD) reactor

Foss Biolab is a pilot plant at Foss dairy farm in Skien, Norway, for nutrient and energy recovery, see Figure 1. Input to the plant is dairy manure, and outputs are high quality fertilizer and biogas consisting of 70-75% methane. The plant is monitored and controlled with a PC-based automation system running LabVIEW.

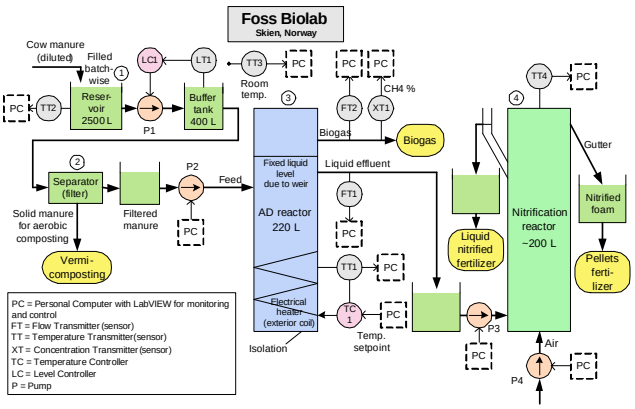

Figure 1: Foss Biolab, Skien, Norway

The main parts of the plant are as follows (the numbers refer to the figure): 1) A reservoir for raw dairy manure containing approximately 25% added water. 2) A separator (filter) to separate the manure into two fractions of similar total solid mass: >70 % of the volume is the wetter fraction and < 30 % is the dryer fraction. 3) A 220 L high rate AD reactor fed with filtered cow manure as substrate for production of energy-rich biogas that contains mainly methane. 4) A 200 L nitrification reactor fed with AD reactor effluent to produce high quality liquid fertilizer and pellets fertilizer from formed foam. The plant has been operational since August 2011.

The present study is about the anaerobic digestion (AD) reactor.

1.3 Outline of this article

The underlying mathematical model of the AD reactor is described in Section 2. Application of the state estimators to the AD reactor is described in Section 3. Conclusions are given in Section 4. The general algorithms of the state estimators used in this study are presented in Appendix A.

1.4 Computing tool

The estimators and simulators are implemented in MATLAB/SIMULINK. The MATLAB Function block in SIMULINK has shown to be very convenient for implementation of the Kalman Filter algorithms and simulators for the AD reactor. Input and output parameters are automatically added to the block as you edit the function header. Both scalars and vectors can be used as inputs and outputs.

2 Hill's anaerobic digestion (AD) model

2.1 Introduction

In 1983, D. T. Hill (Hill, 1983) presented a mathematical model of an anaerobic digestion (AD) process using animal waste as feed. Hill validated the model with real experiments. Features of Hill's model are as follows:

- It is a dynamic model (with differential equations) with the following states: Concentrations

of

  - Biodegradable volatile solids (BVS)
  - Total volatile fatty acid (VFA)
  - Acid-forming micro-organisms
  - Methane-forming micro-organisms

- Different animal wastes can be assumed as feed: Dairy, beef, swine, poultry. These cases differs only in the biodegradability B_0 and the acid factor A_f (all other model parameters being the same).
- VFA-based inhibition is included.
- Washout is included.
- Solids (biomass) retention time can be set larger than the hydraulic retention time (emulating fixed-bed reactors, UASB reactors).
- Temperature-dependency of reaction rates is included.
- Methane gas concentration and flow is calculated.
- The following variables are *not* included in Hill's model: Total biogas flow (but methane gas flow is included, cf. previous point), CO_2, NH_3, alkalinity, pH.

2.2 Modified Hill's model

2.2.1 Differences from original Hill's model

A. Husain (1998) presented Hill's model with more details regarding chemical reactions. Also, Husain changed some of the model parameter values, and the death rate of micro-organisms was modeled as a VFA-based Monod function in stead of as a constant. Husain's modification of Hill's model (Husain, 1998) is used as the basis for the model used in our (the present) study.

In our study we have made the following changes to the model presented in (Husain, 1998). We denote the resulting model "Modified Hill's model".

- Parameters k_1, k_2, k_3, k_4 and k_5, replaces original parameters (yields) $1/Y$, $(1-Y)/Y$, $1/Y_c$, and $k_{meth}(1-Y_c)/Y_c$. These coefficients are estimated (except k_3 which is calculated from the parameter values in the original Hill's model).
- Biodegradable volatile solids (BVS) S_{bvs} is represented with sCOD, not as a fraction of VS.
- Influent VFA, $S_{vfa_{in}}$, is independent of influent BVS, S_{bvs}.
- The Haldane functions in the reaction rates μ and μ_c in Hill's original model are replaced with the simpler Monod functions:

$$\mu = \mu_m(T)\frac{1}{\frac{K_s}{S_{bvs}}+1} \tag{1}$$

$$\mu_c = \mu_{mc}(T)\frac{1}{\frac{K_{sc}}{S_{vfa}}+1} \tag{2}$$

  This makes the calculations with the model easier. Simulations indicate that the omission of the terms S_{vfa}/K_i and S_{vfa}/K_{ic} in the Haldane functions has little impact on the responses under the operating conditions assumed in the present study.
- The Monod functions of the death rates are replaced with constant parameters:

$$K_d = 0.02\ [1/\mathrm{d}] \tag{3}$$

$$K_{dc} = 0.02\ [1/\mathrm{d}] \tag{4}$$

  which is the same way of representing death rates as in ADM1 (Batstone et al., 2002).
- In Hill's original model (Hill, 1983), (Husain, 1998) the retention time of the biomass (here: acidogens and methanogens) is equal to the retention time of the organic material (BVS and VFA) which is equal to the hydraulic retention time:

$$T_d = \frac{V}{F} \tag{5}$$

  However, it is reasonable to assume that the retention time of the biomass is larger than the

retention time of the organic organic material as the biomass to some extent is attached to granules in the reactor, as in a fixed-bed reactor or an UASB reactor. The factor b is here introduced as the ratio between the retention times. Thus, the retention time of the biomass is

$$T_{d_{bact}} = bT_d = \frac{V}{F/b} \tag{6}$$

(In the original Hill's model we would set $b = 1$.) Eq. (6) makes the model coherent with the standard ADM1 model (Batstone, 2002) in this respect, and also with the model presented in (Bernard, 2001) which has been used successfully to model an AD reactor using wine waste as feed.

2.2.2 Nomenclature in modified Hill's model

- F [L/d] is influent or feed flow, which is equal to effluent flow. It is also denoted the load rate.
- V [L] is reactor volume.
- T [^{o}C] is reactor temperature.
- F_{meth} [L CH_4/d] is methane gas flow.
- S_{bvs} [g BVS/L] is concentration of biodegradeable volatile solids (BVS) in the reactor.
- S_{vfa} [g VFA/L] is concentration of volatile fatty acids (VFA) in the reactor.
- X_{acid} [g organism/L] is concentration of acid-forming micro-organisms.
- X_{meth} [g organism/L] is concentration of methane-forming micro-organisms.
- Y_c [g organism/g VFA] is yield coefficient of methane-forming micro-organisms.
- T_d [d] is hydraulic retention time:

$$T_d = \frac{V}{F} \tag{7}$$

where V [L] is reactor volume and F [L/d] is flow = inflow = outflow.

- Retention time factor b which defines the ratio of the hydraulic retention time to the biomass retention time:
- $T_{d_{bact}}$ is the retention time of micro-organisms (biomass):

$$b = \frac{T_{d_{bact}}}{T_d} = \frac{V/F}{V/(F/b)} \tag{8}$$

- k_{meth} [unit one] is a methane gas factor.
- μ [d^{-1}] is growth rate of acid forming micro-organisms.
- $\mu_m(T)$ [d^{-1}] is the temperature-dependent maximum growth rate for acid-forming micro-organisms.
- μ_c [d^{-1}] is growth rate of methane forming micro-organisms.
- $\mu_{mc}(T)$ [d^{-1}] is the maximum growth rate for methane-forming micro-organisms.
- K_s [g BVS/L] is Monod half-velocity constant for acid-forming micro-organisms.
- K_{sc} [g VFA/L] is Monod half-velocity constant for methane-forming micro-organisms.
- K_d [d^{-1}] is specific death rate of acid-forming micro-organisms
- K_{dc} [d^{-1}] is specific death rate of methane-forming micro-organisms

2.2.3 Model equations in modified Hill's model

The modified Hill's model is as follows. The differential equations stems from mass balances of the pertinent components.

$$\dot{S}_{bvs} = (S_{bvs_{in}} - S_{bvs})\frac{F}{V} - \mu k_1 X_{acid} \tag{9}$$

$$\dot{S}_{vfa} = (S_{vfa_{in}} - S_{vfa})\frac{F}{V} + \mu k_2 X_{acid} - \mu_c k_3 X_{meth} \tag{10}$$

$$\dot{X}_{acid} = \left(\mu - K_d - \frac{F/b}{V}\right) X_{acid} \tag{11}$$

$$\dot{X}_{meth} = \left(\mu_c - K_{dc} - \frac{F/b}{V}\right) X_{meth} \tag{12}$$

$$F_{meth} = V \underbrace{\mu_c k_{meth} \frac{1 - Y_c}{Y_c} k_4}_{k_5} X_{meth} = V \mu_c k_5 X_{meth} \tag{13}$$

where

$$\mu = \mu_m \frac{1}{\frac{K_s}{S_{bvs}} + 1} \tag{14}$$

$$\mu_c = \mu_{mc} \frac{1}{\frac{K_{sc}}{S_{vfa}} + 1} \tag{15}$$

where the maximum reaction rates are functions of the reactor temperature as follows:

$$\mu_m(T) = \mu_{mc}(T) = 0.013T - 0.129$$

for $20°\text{C} < T < 60°\text{C}$.

2.2.4 Known parameters in modified Hill's model

The following model parameters have known values:

- Reactor volume:

$$V = 220 \text{ L} \tag{17}$$

- The micro-organisms death rates are given the same values as in the ADM1 model (Batstone et al., 2002):

$$K_d = 0.02 \text{ d}^{-1} \tag{18}$$

$$K_{dc} = 0.02 \text{ d}^{-1} \tag{19}$$

- The "VFA-related" half-velocity constant for methane-forming micro-organisms is assumed to have the same value as in (Husain, 1998):

$$K_{sc} = 3 \text{ g VFA/L} \tag{20}$$

- The ratio between the concentration of the acidogenic micro-organisms and the methanogenic micro-organisms are assumed to be fixed, and equal to

$$r_{am} = \frac{X_{acid}}{X_{meth}} = 0.34 \tag{21}$$

  This ratio is found from simulations of the original Hill's model (Hill, 1983) which reveals that the ratio is varying slightly around 0.34 in quite different operating conditions.

- Yield coefficient of methane-forming micro-organisms:

$$Y_c = 0.0315 \text{ g organism/g VFA} \tag{22}$$

- Methane gas factor:

$$k_{meth} = 0.5 \text{ [unit one]} \tag{23}$$

2.2.5 Adaptation of modified Hill's model using real data

The following model model parameters in modified Hill's model have unknown values and are thus to be estimated:

- Reaction parameters (yield parameters) k_1, k_2, k_3, k_4, and k_5.
- Half-velocity Monod-constant for acid-forming micro-organisms, K_s.
- Retention time factor, b.

These parameters were estimated using offline-data from laboratory analysis and online-data from sensors. Offline-data used are sCOD and total VFA. Online-data used are feed flow (loading rate), reactor temperature, biogas flow, and methane gas concentration. (The latter two provides methane gas flow.) The time series selected for model adaptation starts at $t = 44$ d (26. Sept. 2011) and ends at $t = 63$ (15. Oct. 2011). 13. August 2011 is the reference point of time, i.e. $t = 0$ d at that time. (The state estimators will however be applied to a larger (longer)

time series, ending at $t = 149$ d.) Figure 2 shows this time series. The pertinent time interval was selected to include variations of both feed flow and reactor temperature. In the upper plot are the real feed flow and reactor temperature. In the lower plot the blue curve represents the produced methane gas flow. The red curve in the lower plot represents the simulated methane gas flow using the adapted model. The simulation is commented in Sec. 2.2.6.

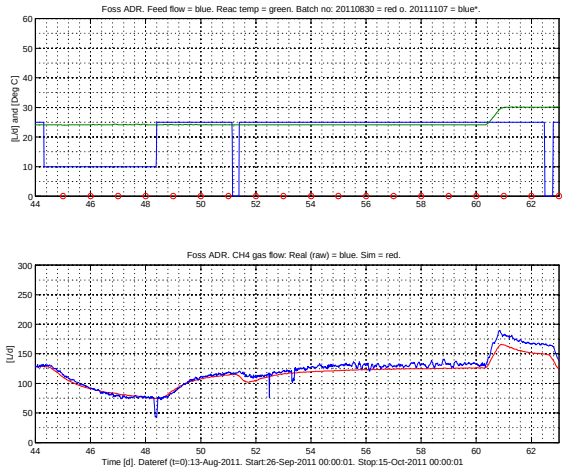

Figure 2: Upper plot: Real feed flow and reactor temperature. Lower plot: Real and simulated produced methane gas flow. The sudden stops in the feed flow are due to blockings.

The gas flow time series shown in Figure 2 has some large outliers. These ouliers are caused by power outage and/or gas blocking. Such outliers can cause problems for controllers and estimators. Removal of outliers is described in Section 3.2.2.

The model was adapted using data from both a steady-state operating point at $t = 44$ d applied to a steady-state version of the model (to get rid of the time-derivatives in the model) *and* by adjusting parameter k_4 in iterated simulations so that simulations with the dynamic model correspond well to the dynamic responses from $t = 44$ to 63 d. In this way *both* steady-state data and dynamic data are exploited for model adaptation in a simple way.

In the pertinent operating point ($t = 44$ d) used for parameter estimation, the model variables have the following values:

- Feed flow:
$$F = 25 \text{ L/d} \tag{24}$$
- Reactor temperature:
$$T = 24.1 \ ^{\text{o}}\text{C} \tag{25}$$
- Influent and effluent concentrations of BVS in terms of sCOD as found in laboratory analysis:
$$S_{bvs_{in}} = 13.4 \text{ g sCOD/L} \tag{26}$$
$$S_{bvs} = 4.45 \text{ g sCOD/L} \tag{27}$$
- Influent and effluent concentrations of (total) VFA as found in laboratory analysis:
$$S_{vfa_{in}} = 3.40 \text{ g/L} \tag{28}$$
$$S_{vfa} = 0.407 \text{ g/L} \tag{29}$$
- Methane gas flow F_{meth} (given as the product of total biogas flow F_{biogas} – detected with an online gas flow sensor – and methane concentration c_{meth} detected with an online gas concentration sensor):
$$F_{meth} = 128 \text{ L/d} \tag{30}$$

The results of parameter estimation are as follows:

$$\hat{b} = 56.6 \tag{31}$$
$$\hat{K}_s = 32.8 \tag{32}$$
$$k_3 = 31.7 \tag{33}$$
$$k_4 = 1.60 \tag{34}$$
$$k_5 = 24.6 \tag{35}$$
$$\hat{X}_{meth} = 1.07 \tag{36}$$
$$\hat{X}_{acid} = X_{meth} r_{am} = 3.65 \tag{37}$$
$$\hat{k}_1 = 12.7 \tag{38}$$
$$\hat{k}_2 = 5.11 \tag{39}$$

2.2.6 Simulated vs. measured responses

In Figure 2, the red curve in the lower plot represents the simulated methane gas flow using the adapted model. The initial state for the simulation is set equal to the steady-state values at $t = 44$ which are (27), (29), (36) and (37). The model apparently represents important dynamic properties of the real reactor after that period. In subsequent time interval the model does not fit that well, but this is to be expected since we input and environmental conditions change. Particularly, from around $t = 84$ d, the reactor started to behave apparently abnormally with a declining gas production for approximately 15 days. However, this interval, too, is included in the data set applied with state estimation in this report.

3 Application of state estimators to the AD reactor

In the subsequent sections various state estimators are applied to both a simulated and the real AD reactor.

3.1 Selection of ultimate estimator from simulation study

In this section various estimators will be compared in a simulation study. The purpose is to get a basis for selecting the most proper estimator to be applied to the real AD reactor.

The list below shows the estimators which are compared. A detailed description of each of the estimator are given in the referred section (in the Appendix).

- Simulation-estimator, cf. Section A.3.
- Ordinary Unscented Kalman Filter (UKF) with no augmentation, cf. Section A.5. The state vector is

$$\begin{aligned} x &= [S_{bvs}, S_{vfa}, X_{acid}, X_{meth}]^T \quad (40) \\ &= [x_1, x_2, x_3, x_4]\,T \end{aligned}$$

  The control variable (manipulating variable) is

$$u = \left[\ F\ \right] = \left[\ u_1\ \right] \quad (41)$$

  The measurement (process output) is

$$y = \left[\ F_{meth}\ \right] = \left[\ y_1\ \right] \quad (42)$$

- Ordinary Extended Kalman Filter (EKF): Same state vector as for ordinary UKF (see above).
- Augmented UKF with $S_{vfa_{in}}$ as augmentation state, cf. Sections A.5 and A.6. The state vector is

$$\begin{aligned} x &= [S_{bvs}, S_{vfa}, X_{acid}, X_{meth}, S_{vfa_{in}}]^T \quad (43) \\ &= [x_1, x_2, x_3, x_4, x_5]\,T \end{aligned}$$

  u and y are as above.
- Augmented EKF: Same state vector as for Augmented UKF (see above).

In the simulations presented in the following the initial state of both the "real" reactor and the estimators corresponds to the approximately steady-state operating point of day 44 in Figure 2. Values of parameters and states are as presented in Sections 2.2.4 and 2.2.5.

The ordinary EKF and UKF are equally tuned, i.e. $x_{apost}(t_0)$, $P_{apost}(t_0)$, Q and R are the same for the two estimators. Also, the augmented EKF and UKF are equally tuned.

The challenge to the estimators is to estimate the states when there is a model error related to VFA concentration of the feed, $S_{vfa_{in}}$. At the selected operating point we have from lab analysis that

$$S_{vfa_{in_0}} = 3.40 \text{ g/L} \quad (44)$$

This value is used for $S_{vfa_{in}}$ in the various state estimators. To impose a model error it is assumed that the "real" (correct) value is

$$\begin{aligned} S_{vfa_{in_{\text{real}}}} &= S_{vfa_{in_0}} + \Delta S_{vfa_{in}} \quad (45) \\ &= 3.40 \text{ g/L} + 2 \text{ g/L} \quad (46) \\ &= 5.40 \text{ g/L} \quad (47) \end{aligned}$$

$S_{vfa_{in}}{}_{\text{real}}$ is used in the simulator representing the real reactor, while $S_{vfa_{in}}{}_{0}$ is used in the state estimators.

Figures 3 – 6 shows results of a simulation from $t =$ 0 to 2 days with the various state estimators. The feed flow F is constant at 25 L/d, and the reactor temperature is constant at 24.1 ^{o}C.

- Figure 3 shows the estimates of the states $S_{bvs} = x_1$ and $S_{bvs} = x_1$.
- Figure 4 shows the estimates of the states $X_{acid} = x_3$ and $X_{meth} = x_4$.
- Figure 5 shows the estimate of the augmentation state, $S_{vfa_{in}} = x_5$.
- Figure 6 shows the Kalman Filter gains for the augmented EKF and the augmented UKF.

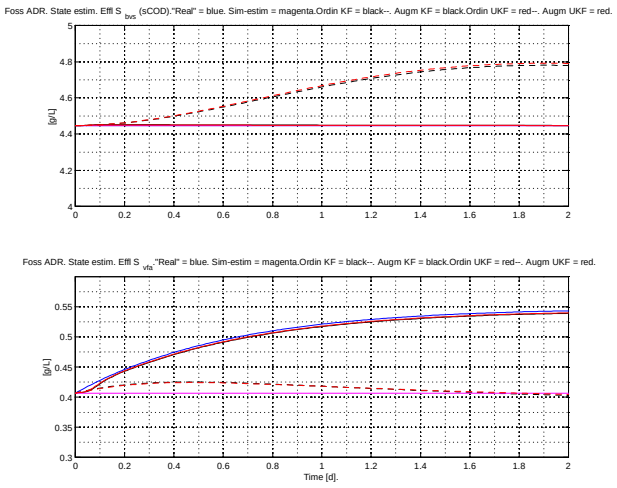

Figure 3: State estimation of simulated AD reactor: $S_{bvs} = x_1$ and $S_{vfa} = x_2$.

Below are comments to the plots shown in Figures 3 – 6.

- Figures 3 and 4 show that the state estimation errors are relatively small with the augmented

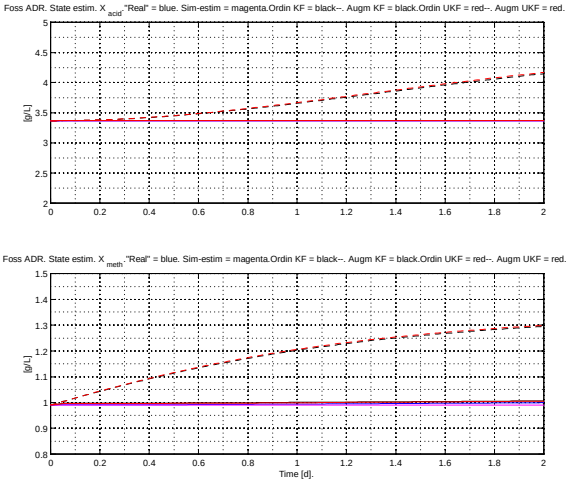

Figure 4: State estimation of simulated AD reactor: $X_{acid} = x_3$ and $X_{meth} = x_4$.

EKF and UKF. With the non-augmented EKF and UKF estimators the state estimation errors are large. One explanation is that the estimation errors in the ordinary states kind of compensates for the model error regarding $S_{vfa_{in}}$. This "compensating" state estimation error can be even larger than the state estimation error present with the simulation-estimator. This is demonstrated in Figure 7 where the system is simulated for 50 days.

- Figure 5 shows that the augmented EKF and UKF estimates the partly unknown parameter $S_{vfa_{in}}$ relatively well.

  It is interesting to observe that the EKF and the UKF performs very similarly (they are tuned equally).

  The estimation of parameter $S_{vfa_{in}}$ is apparently beneficial also for the estimation of the "original" states, S_{bvs}, S_{vfa}, X_{acid} and X_{meth} since with the augmented estimators the estimation errors for these states are small, cf. the previous figures.

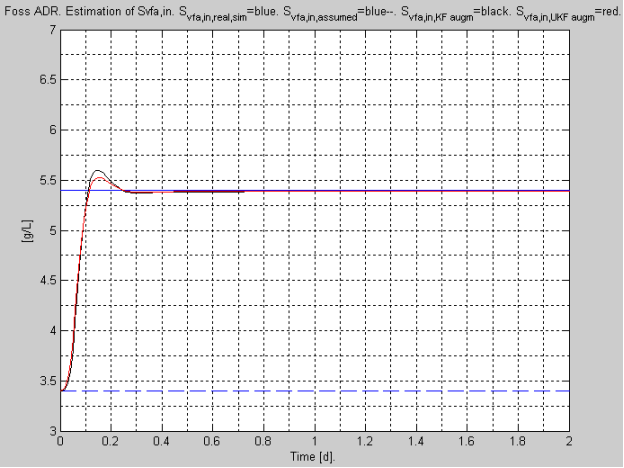

Figure 5: State estimation of simulated AD reactor: VFA concentration in influent, $S_{vfa_{in}} = x_5$ (augmentation state)

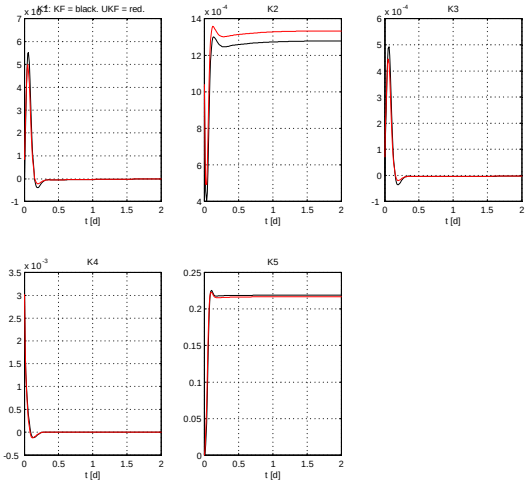

Figure 6: Kalman filter gains for the augmented EKF and the augmented UKF

- Figure 6 shows that the Kalman gains are quite similar in (augmented) EKF and UKF. This is an interesting observation since the mathematical formulas for the Kalman gains are apparently very different.
- Figures 3 – 4 indicate that the performances of ordinary EKF and UKF and of augmented EKF and UKF are similar. In the simulations there are no process noise and no measurement noise. In Example 14.2 in (Simon, 2006) which involves process and measurement noise in a nonlinear system, a significant improvement regarding noise contents in the state estimates is obtained with UKF compared with EKF.

From the results presented above it can be concluded that the two best estimators for the AD reactor, and probably in many other applications too, are the augmented EKF and the augmented UKF. Then, how to select among these two? The UKF is designed to give smaller estimation errors than EKF do for nonlinear systems in the case of random process and measurement noises. The AD reactor model is nonlinear, so it can be assumed that the performance of the UKF is better than of the EKF. In the present study both augmented EKF and augmented UKF has actually been applied to real, noisy data for the AD reactor, but there were no significant difference, probably because the effects process noise and measurement noise are relatively small compared to the effects of model errors.

In addition to the potential benefit related to performance, the UKF is simpler do design and implement since the linearization of the system function and the

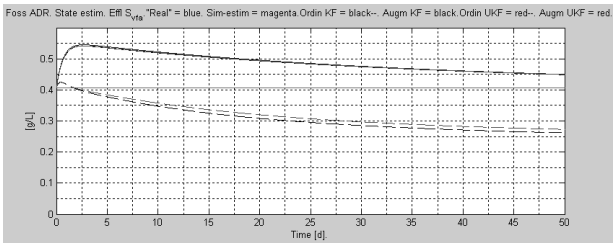

Figure 7: Estimated S_{bvs} and S_{vfa} simulated for 50 days.

measurement function is not needed. (Of course, linearization may be necessary for other reasons, like analysis of dynamics and local stability.)

Consequently, the augmented UKF is selected as the prefered estimator for the AD reactor.

3.2 Application to real reactor

3.2.1 Experimental conditions

In Section 3.1 the augmented UKF was pointed out as the prefered estimator for the AD reactor. The augmentation state was $S_{vfa_{in}}$. However, when applying the UKF to data from the real AD reactor, also the other feed component, $S_{bvs_{in}}$, will be estimated. Hence, the UKF with both $S_{vfa_{in}}$ and $S_{bvs_{in}}$ as augmentation states will be applied. The state vector is

$$\begin{aligned} & x \qquad (48) \\ = \; & [S_{bvs}, S_{vfa}, X_{acid}, X_{meth}, S_{vfa_{in}}, S_{bvs_{in}}]^T \\ = \; & [x_1, x_2, x_3, x_4, x_5, x_6]\, T \end{aligned}$$

All estimators are used with values of real flow, reactor temperature and methane gas flow data from $t = 44$ d (26. Sept. 2011) to 149 d (9. Dec. 2011). However, outliers are removed in the methane gas flow data, cf. Section 3.2.2.

For all estimators the initial values of the original states, S_{bvs}, S_{vfa}, X_{acid} and X_{meth}, as found from the steady-state operating point at $t = 44$ d are as follows:

$$S_{bvs_0} = x_{1_0} = 4.45 \qquad (49)$$

$$S_{vfa_0} = x_{2_0} = 0.407 \qquad (50)$$

$$X_{acid_0} = x_{3_0} = 3.65 \qquad (51)$$

$$X_{meth_0} = x_{4_0} = 1.07 \qquad (52)$$

The augmentation states have the following values at $t = 44$ d:

$$S_{vfa_{in}} = x_{5_0} = 3.40 \qquad (53)$$

$$S_{bvs_{in}} = x_{6_0} = 13.4 \qquad (54)$$

To introduce a model error in the applications, the initial values of both ordinary state variables and augmentation state variables are set to 20% of their known values given above.

3.2.2 Removal of outliers from raw data

Figure 2 shows the time series of feed flow, reactor temperature and methane gas flow which will used with the state estimator. The gas flow contains several outliers caused by power outage and/or gas blocking. Of course, such outliers will cause problems for the estimator since they contain wrong information about the real gas flow.

To remove the outliers a state estimator is used. Of practical reasons, the state estimator used for outlier removal is an ordinary Extended Kalman Filter which is independent of the state estimator(s) used in other parts of the experiments described in the following sections. This is because in some of the experiments, the (other) state estimators will produce "wild" estimates. The original (raw) measurement is substituted by the estimated measurement if the absolute value of the difference between the original measurement and the estimate is larger than a certain value, which here is set to 10 L/d (methane flow). Figure 8 shows the positive result of the outlier removal.

3.2.3 Tuning the state estimator

The tuning parameters of the Unscented Kalman Filter are $x_{apost}(t_0)$, $P_{apost}(t_0)$, Q and R (these parameters are defined in Appendix A.5). Of course, ideally these parameters are set equal to their known values. But, in practice these values are not known particularly well, except perhaps $x_{apost}(t_0)$ and R. Good guidelines are hard to find. Even a thorough book as (Simon, 2006) gives little advice. In the present study the following tuning procedure has been used.

- Initial estimated state $x_{apost}(t_0)$ is set according to a qualified guess which should be (49) – (54). However, to introduce a model error in the application, all the initial states are set to 20% of their assumed known values (49) – (54).
- Initial state estimation error covariance

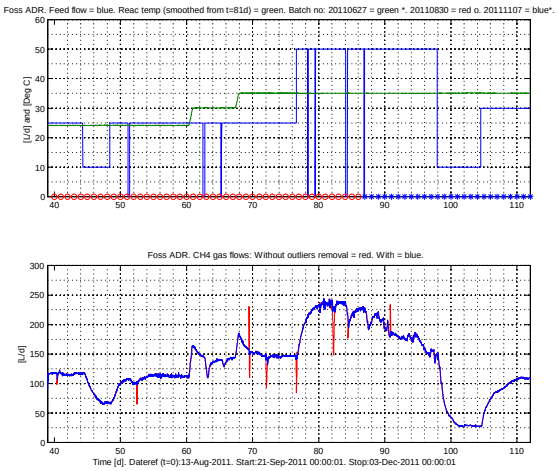

Figure 8: Gas flow measurement - without and with outlier removal

$P_{apost}(t_0)$ is an n x n-matrix commonly set as a diagonal matrix. In lack of other options we can try setting the covariance of the estimation error for state variable i equal to a constant times the square of the guessed initial state variable $x_{i_{apost}}(t_0)$:

$$P_{apost}(t_0)_{i,i} = \left[k_i x_{i_{apost}}(t_0)\right]^2 \tag{55}$$

In the present study it is found by trial-and-error that

$$\{k_i\} = \{1, 1, 1, 1, 1, 5\} \tag{56}$$

To be consistent with the assumptions about model errors in the state variables, $x_{apost}(t_0)$ is here set equal to 20% of (49) – (54).

- Process noise covariance Q is in general a time-varying n x n diagonal matrix, but it is usually set to a constant matrix. Assuming a continuous-time estimator, it makes sense to try relating the diagonal elements (prosess noise variances) for the continuous-time noise covariance matrix to the magnitude of the pertinent state variables in the same way as for P_{apost} above. However, we can assume that the noise constitutes only a fraction of the state variable:

$$Q_{c_{i,i}} = \left[l_i x_{i_{apost}}(t_0)\right]^2 \tag{57}$$

In the present study it is found by trial-and-error that

$$\{l_i\} = \{8, 4, 4, 2, 10, 10\} \tag{58}$$

To be consistent with the assumptions about model errors in the state variables, $x_{apost}(t_0)$ is here set equal to 20% of (49) – (54).

The UKF we use is a discrete-time estimator. Therefore, we can use the following relation between the continuous-time process noise covariance Q_c and the discrete-time process noise covariance Q assuming the sampling time is T_s (Simon, 2006):

$$Q = Q_c T_s \tag{59}$$

One benefit of using the continuous-time covariance in the tuning of the UKF, is that the tuning becomes more or less independent on the sampling-time.

- Measurement noise covariance R is in general a time-varying m x m matrix, but is usually set to a constant matrix. For a continuous-time estimator, diagonal element number j can be estimated from a representative time-series of the measurement y_j:

$$R_{c_{j,j}} = \mathrm{var}\left(y_j\right) \tag{60}$$

To find the corresponding R for a discrete-time estimator, we can use the following relation (Simon, 2006):

$$R = \frac{R_c}{T_s} \tag{61}$$

From a representative portion of the real time series for the AD reactor, it was found that

$$R_c = \mathrm{var}(y) = \mathrm{var}(F_{meth}) = 1.44 \tag{62}$$

Assuming that $x_{apost}(t_0)$, $P_{apost}(t_0)$ and R have been set from estimated or observed signal values, Q_c remains as the tuning parameter:

- Increasing $Q_{c_{i,i}}$ makes the estimate for state variable x_i converge faster to the assumed true value, but with the drawback that the estimate for x_i becomes more noisy (caused by the increased propagation of the measurement noise, via the Kalman Filter gain(s)).
- Reducing $Q_{c_{i,i}}$ has the opposite effects.

The numerical values of the tuning parameters used in the actual application to the AD reactor are not presented here since sufficient information about the tuning is given above.

3.2.4 Results and discussions

Figures 9 – 12 show estimated responses and measurements (from online sensors and laboratory analyses). The estimators use are:

- Unscented Kalman Filter with values of initial states and tuning parameter as given in the previous sections.
- Simulation-estimator which is simply a simulator using the same model and the same initial state values as the UKF does. The reason for showing responses with the simulation-estimator is to demonstrate benefits or drawbacks by using an advanced, feedback-based estimator as UKF. After all, the simulation-estimator is vastly simpler than the UKF, and requires no tuning except for setting a proper initial state.

Comments and discussions to the results are given in the following.

- Figure 9 shows in the upper plot the feed flow and the reactor temperature and in the lower plot the measured and estimated methane gas flow.

  The UKF estimates the gas flow accurately, but it is typical for well-tuned error-driven estimators that the measurement is estimated accurately.

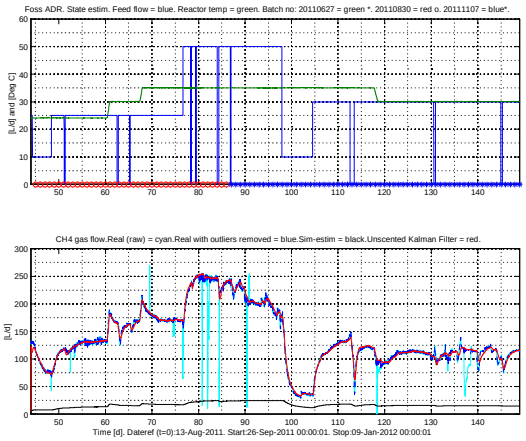

Figure 9: Upper: Measured feed flow and reactor temperature. Lower: Measured and estimated methane gas flow

  The simulation-estimator gives a very poor estimation of the methane gas, which is at least due to the imposed model error (in the initial state estimate, including the feed concentrations of BVS and VFA).

- Figure 10 shows measurements and estimates of the states $S_{bvs} = x_1$ and $S_{vfa} = x_2$.

  The UKF underestimates S_{bvs}, particularly after approximately $t = 97$ d. The underestimation *may* indicate that only a part of the sCOD detected in lab analysis constitues the substrate for the biomass (microbes). This is an interesting observation in itself because it indicates that state estimators can be used to identify the fraction of other, alternative substrate measures, like TS, VS, TSS and VSS, which is used a substrate for the biomass.

  The increased underestimation of S_{bvs} after $t = 97$ d *may* stem from the fact that a new batch of manure was taken into use at $t = 87$ d, and according to the farmer this batch has a smaller biogas production potential since it is fresher than the previous batch.

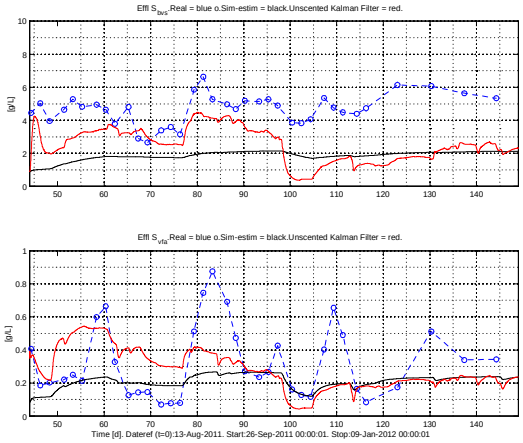

Figure 10: Measurements and estimates of the states $S_{bvs} = x_1$ and $S_{bvs} = x_1$.

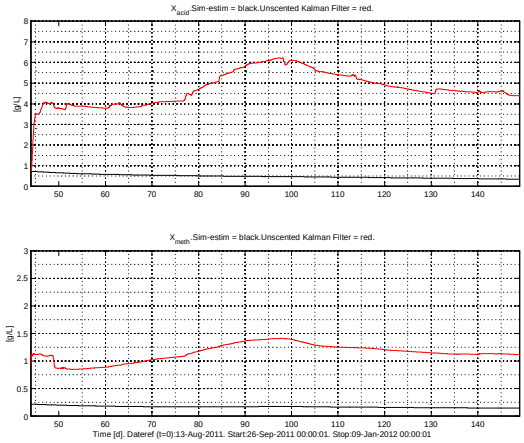

Figure 11: Estimates of the states $X_{acid} = x_3$ and $X_{meth} = x_4$.

The UKF estimates S_{vfa} to some degree. The peaks and bottoms of the measurements are not resembled, although their changes are somewhat resembled.

For both S_{bvs} and S_{vfa} the simulation-estimator gives estimates which may be useful. It is difficult to evaluate the accuracy of these estimates.

Neither of the estimators resembles the clear peaks in the analysis values. It is not clear if these peaks are due to analysis errors or real values, or poor sampling procedures.

- Figure 11 shows estimates for states $X_{acid} = x_3$ and $X_{meth} = x_4$. Since we do not have any lab analysis of the biomass concentrations, X_{acid} and X_{meth}, it is difficult to determine the accuracy of the estimates. However, the UKF gives estimates which are much closer to the calculated values (51) – (52).

- Figure 12 shows estimates of the augmentation states $S_{vfa_{in}} = x_5$ and $S_{bvs_{in}} = x_6$. We do not know the reason for the big, abrupt variations of the measurements of $S_{vfa_{in}}$.

  The simulation-estimator is of course not able to estimate any other value of $S_{vfa_{in}}$ and $S_{bvs_{in}}$ than is used as an input signal (parameter) in the estimator, so the estimation is large, as expected.

  UKF resembles quite well the measurements, despite the large errors imposed on the initial values of the estimates. $S_{bvs_{in}}$ seems to be somewhat underestimated after $t = 97$ d, but the reason may be the same as for the underestimation of S_{bvs} as explained above.

- Although not shown with plots in this article, the Extended Kalman Filter produced results comparable with the Unscented Kalman Filter. However, it was much easier to do the necessary changes with the UKF when trying out various models (augmentations). This is because the linearization step is not needed in the UKF.

4 Conclusions

- The modified Hill's model can represent a real AD reactor (based on cow manure as substrate) with sufficient accuracy to constitute the basis for state estimators for the reactor.

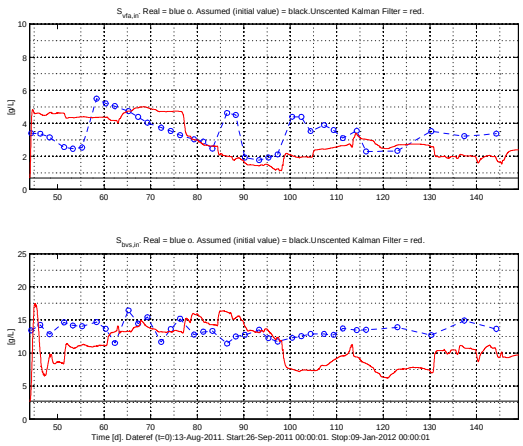

Figure 12: Measurements and estimates of the augmentation states, $S_{vfa_{in}} = x_5$ and $S_{bvs_{in}} = x_6$.

- The Unscented Kalman Filter (UKF) is an attractive alternative to the Extended Kalman Filter (EKF) mainly because it is much easier to make the necessary changes in the algorithm when various models are to be tried, because the calculation of Jacobi matrices for linearization is not needed.

- In general, the UKF has the potential of improving the estimates compared with EKF. With the real data used in this project the results with (augmented) EKF are almost the same as with UKF.

- The robustness against (imposed large) modeling errors are greatly improved by augmenting the state estimator with state variables representing more-or-less unknown parameters or input signals. Augmenting the state estimators with (unknown) feed concentrations $S_{bvs_{in}}$ and $S_{vfa_{in}}$ is particularly beneficial since it improves the estimates of the other state variables (this was demonstrated in a simulation study).

- Estimation of feed concentrations $S_{bvs_{in}}$ and $S_{vfa_{in}}$ can be valuable in itself as their values can be used to predict the gas production of the reactor and to indicate if the feed quality is increasing or decreasing.

- Since the prosess output (measurement) is predicted accurately in error-driven estimators (UKFs), this prediction can replace measurement outliers which increases the robustness of the system in monitoring and control applications.

Acknowledgement

Financial support to this research is provided by Telemark University College (TUC), Norway. Thanks to K. Vasdal and E. Fjelddalen, and to a number of students at TUC, for practical support.

A State estimator algorithms

A.1 Introduction

In this study a number of state estimators are applied to simulated data and measured data from the physical reactor. The estimators are ordinary and augmented Extended Kalman Filters and ditto Unscented Kalman Filters (Simon, 2006), and a simulation-estimator (a ballistic or open-loop estimator). All estimators are based on a modified version of a first principles model of the reactor with four state variables originally developed by D. T. Hill (1983). The model has been adapted to the AD reactor using a data set from online sensors and lab analysis. The estimators are compared with respect to accuracy of the means of the estimates, noise suppression in the estimates, robustness against model errors, estimator tuning, and implementation issues.

In the following sections, the state-space model form used in the estimators is defined. Then the state estimator algorithms are presented.

A.2 State-space model form

The various state estimator algorithms described in this chapter are assumed to have the following form (the notation mainly follows (Simon, 2006)):

$$x(t_{k+1}) = f\left[x(t_k), u(t_k)\right] + w(t_k) \tag{63}$$

$$y(t_k) = h[x(t_k)] + v(t_k) \tag{64}$$

f is the system function. h is the measurement or process output function. x is the state variable (vector). u is the process input (vector) having known value. It includes control signals and known process disturbances. y is the process measurement (vector). w is the random process noise, or disturbance (vector):

$$w(t_k) \sim [0, Q(t_k)] \text{ (mean is 0; covariance is } Q) \tag{65}$$

v is the random measurement noise (vector):

$$v(t_k) \sim [0, R(t_k)] \text{ (mean is 0; covariance is } R) \tag{66}$$

f and h are vector functions (linear or nonlinear).

Typically, the above model, (63) – (64), stems from discretizing the continuous-time model (subindex c for continuous-time)

$$\dot{x}(t) = f_c\left[x(t), u(t)\right] + w_c(t) \tag{67}$$

$$y(t) = h[x(t)] + v_c(t) \tag{68}$$

with a proper discretization method. (w and v are now actually continuous-time noise signals.) We will use the Explicit Euler method with time-step T_s [d]. This is a simple method which can be applied to nonlinear systems. With T_s sufficiently small, the behaviour of the discrete-time system will be very equal to the original continuous-time system. Discretizing (67) with the Explicit Euler method, and avoiding expressing the details about the discretization of continuous-time random signals, the resulting discrete-time model is

$$x(t_{k+1}) = \underbrace{x(t_k) + T_s f_c\left[x(t_k), u(t_k)\right]}_{f[x(t_k), u(t_k)]} + w(t_k) \tag{69}$$

$$y(t_k) = h[x(t_k)] + v(t_k) \tag{70}$$

A.3 Simulation-estimator

The simplest state estimator is simply a simulator running in parallel (synchroneously) with the real system. This estimator will here be denoted *simulation-estimator*. The simulated states are used as state estimates, and they are *not* adjusted in any way. (In a Kalman Filter the estimates are adjusted continuously based on the difference between the real and the predicted (simulated) measurement.) The simulation-estimator can also be denoted an open-loop estimator. Another term is ballistic[1] estimator. The simulation-estimator is actually the only option if there are no reliable measurements available for correcting the estimates.

The algorithm of the simulation-estimator state estimator uses the model (69) – (70) directly, but since the noise signals w and v are random with zero mean, they are not included in the simulation algorithm. Hence, the simulation-estimator is

$$\begin{aligned} x_e(t_{k+1}) &= f\left[x_e(t_k), u(t_k)\right] && (71)\\ &= x_e(t_k) + T_s f_c\left[x_e(t_k), u(t_k)\right] && (72)\\ &\quad \text{(assuming Explicit Euler)} \end{aligned}$$

$$y_e(t_k) = h[x_e(t_k)] \tag{73}$$

Figure 13 shows a block diagram depicting this state estimator.

A.4 Extended Kalman Filter

The Extended Kalman filter (EKF) is an extension of the basic Kalman filter suitable for nonlinear systems. Assuming the model is (69) – (70), the EKF algorithm is as follows (Simon, 2006).

- Initial step[2] ($k = 0$):
  - Aposteriori state estimate:

$$x_{apost}(t_0) = E\left(x_0\right) \tag{74}$$

[1] Since it moves in the state space without any correction, just driven by its own dynamics.

[2] E is expectation.

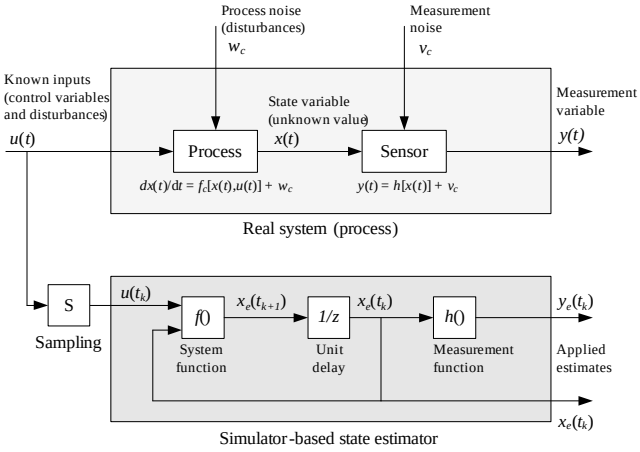

Figure 13: Simulator-estimator

– Covariance of estimation error:

$$P_{apost}(t_0) = E\left\{ \begin{array}{l} [x(t_0) - x_{apost}(t_0)] \cdot \\ [x(t_0) - x_{apost}(t_0)]^T \end{array} \right\} \tag{75}$$

For time steps $k = 1, 2, 3,...$:

1. Partial derivative of system function (Jacobian matrix):

$$F(t_{k-1}) = \left.\frac{\partial f}{\partial x}\right|_{x_{apost}(t_{k-1}),u(t_{k-1})} \tag{76}$$

$$= I + T_s \left.\frac{\partial f_c}{\partial x}\right|_{x_{apost}(t_{k-1}),u(t_{k-1})} \tag{77}$$

2. Time-updates:

   (a) Apriori estimate (predicted estimate):

$$x_{apri}(t_k) = f\left[x_{apost}(t_{k-1}), u(t_{k-1})\right] \tag{78}$$

$$= x_{apost}(t_{k-1}) + T_s f_c\left[x_{apost}(t_{k-1}), u(t_{k-1})\right] \tag{79}$$

   (b) Covariance of estimation-error:

$$P_{apri}(t_k) = F(t_{k-1}) P_{apost}(t_{k-1}) F(t_{k-1})^T + Q \tag{80}$$

3. Partial derivative of output function (Jacobian matrix):

$$H(t_k) = \left.\frac{\partial h}{\partial x}\right|_{x_{apri}(t_k),u(t_k)} \tag{81}$$

4. Measurement updates:

   (a) Kalman filter gain:

$$K(t_k) = P_{apri}(t_k) H(t_k)^T \cdot \left[H(t_k) P_{apri}(t_k) H(t_k)^T + R\right]^{-1} \tag{82}$$

   (b) Measurement estimate:

$$y_{apri}(t_k) = h[x_{apri}(t_k)] \tag{83}$$

   (c) Innovation variable[3]:

$$e\left(t_k\right) = y(t_k) - y_{apri}(t_k) \tag{84}$$

   (d) *State estimate (aposteriori estimate, or corrected estimate), which is used as the applied estimate, x_e:*

$$x_e(t_k) = x_{apost}\left(t_k\right) = x_{apri}\left(t_k\right) + K(t_k) e\left(t_k\right) \tag{85}$$

   (e) Covariance of estimation-error:

$$P_{apost}(t_k) = \left[I - K(t_k) H(t_k)\right] P_{apri}(t_k) \tag{86}$$

A.5 Unscented Kalman Filter

The Unscented Kalman Filter (UKF) is an extension of the basic Kalman Filter suitable for nonlinear systems (Julier et al., 1997). The core principle behind UKF is that the propagation of the mean and the covariance of the state estimates is calculated using the nonlinear model directly. This is different from the Extended Kalman Filter (EKF) where the propagation of the covariance is calculated from the linearized model. In UKF, the propagation of the mean and covariance are calculated from so-called

[3] Also denoted the innovation process.

sigma points which are a number of points in the state space "around" the present state estimate. The distance between the current state estimate and the sigma points are calculated from present state estimate covariance. The optimal estimate is calculated as an average of the sigma points.

Comparing UKF with EKF:

- The propagation (prediction) of the mean and covariance of the estimation error is more accurate with UKF, and therefore the estimates can also be more accurate because more accurate covariance information is used in the calculation of the estimates.
- No linearization is needed in UKF. So, you do not have to calculate the Jacobians of the system function and the measurement function in UKF, while this is necessary in EKF. This is a great practical benefit when you are trying out various models for the estimator, like when you try various augmentations of the state vector.
- The computational burdens are not much different.

Thus, the UKF has benefits related to both performance and design.

There are a number of alternative UKF algorithms, with different complexity and parameters to be selected by the user (Simon, 2006). Assuming the model is (69) – (70), the basic UKF algorithm can be stated as follows. The algorithm is as given in (Simon, 2006), but with somewhat different notation.

- Initial step[4] ($k = 0$):
  - Aposteriori state estimate:
$$x_{apost}(t_0) = E\left(x_0\right) \tag{87}$$
  - Covariance of estimation error:
$$P_{apost}(t_0) = E\left\{ \begin{array}{c} [x(t_0) - x_{apost}(t_0)] \cdot \\ [x(t_0) - x_{apost}(t_0)]^T \end{array} \right\} \tag{88}$$

[4] E is expectation.

For time steps $k = 1, 2, 3,...$:

1. Time-updates:
   (a) Calculate $2n$ sigma points (n is the number of states) based on the available aposteri estimate:
$$x_\sigma^{(i)}(t_{k-1}) = x_{apost}(t_{k-1}) + x^{(i)T},\ i = 1, \ldots, 2n \tag{89}$$
$$x^{(i)} = \left(\sqrt{nP_{apost}(t_{k-1})}_i\right)^T,\ i = 1, \ldots, n \tag{90}$$
$$x^{(i+n)} = -\left(\sqrt{nP_{apost}(t_{k-1})}_i\right)^T,\ i = 1, \ldots, n \tag{91}$$
   where $\sqrt{}$ means matrix square root, and sub index i means i'th row.
   (b) Propagate the sigma points using the (discrete-time) system function f (below, f_c is the continuous-time system function):
$$\begin{aligned} & x_\sigma^{(i)}(t_k) && (92)\\ = \ & f\left[x_\sigma^{(i)}(t_{k-1}), u(t_{k-1})\right] && (93)\\ = \ & x_\sigma^{(i)}(t_{k-1}) && (94)\\ & + T_s f_c\left[x_\sigma^{(i)}(t_{k-1}), u(t_{k-1})\right] && (95)\\ & \text{(Explicit Euler)} \end{aligned}$$
   (c) Calculate the apriori state estimate as the mean values of the propagated, transformed sigma points:
$$x_{apri}(t_k) = \frac{1}{2n}\sum_{i=1}^{2n} x_\sigma^{(i)}(t_k) \tag{96}$$
   (d) Calculate the apriori state covariance:
$$\begin{aligned} & P_{apri}(t_k) && (97)\\ = \ & \frac{1}{2n}\sum_{i=1}^{2n}\left[x_\sigma^{(i)}(t_k) - x_{apri}(t_k)\right] && (98)\\ & \left[x_\sigma^{(i)}(t_k) - x_{apri}(t_k)\right]^T && (99)\\ & + Q(t_k) && (100) \end{aligned}$$

2. Measurement updates:

   (a) Calculate $2n$ sigma points (n is the number of states) based on the available apriori estimate:

$$x_\sigma^{(i)}(t_{k-1}) = x_{apost}(t_{k-1}) + x^{(i)T},\ i = 1, \ldots, 2n \tag{101}$$

$$x^{(i)} = \left(\sqrt{nP_{apost}(t_{k-1})}_i\right)^T,\ i = 1, \ldots, n \tag{102}$$

$$x^{(i+n)} = -\left(\sqrt{nP_{apost}(t_{k-1})}_i\right)^T,\ i = 1, \ldots, n \tag{103}$$

   where $\sqrt{}_i$ means matrix square root, and sub index i means i'th row.

   (b) Transform the state estimate sigma points to corresponding measurement "sigma points" using the measurement function h:

$$y_\sigma^{(i)}(t_k) = h[x_\sigma^{(i)}(t_k)] \tag{104}$$

   (c) Calculate the predicted measurement estimate as the mean values of the transformed measurement "sigma points":

$$y_{pred}(t_k) = \frac{1}{2n}\sum_{i=1}^{2n} y_\sigma^{(i)}(t_k) \tag{105}$$

   (d) Estimate the covariance of the predicted measurement:

$$\begin{aligned} & P_y(t_k) && (106)\\ = & \frac{1}{2n}\sum_{i=1}^{2n}\left[y_\sigma^{(i)}(t_k) - y_{pred}(t_k)\right] && (107)\\ & \left[y_\sigma^{(i)}(t_k) - y_{pred}(t_k)\right]^T && (108)\\ & + R(t_k) && (109)\end{aligned}$$

   (e) Estimate the cross covariance between apriori state estimate and predicted measurement:

$$\begin{aligned} & P_{xy} && (110)\\ = & \frac{1}{2n}\sum_{i=1}^{2n}\left[x_\sigma^{(i)}(t_k) - x_{apri}(t_k)\right] && (111)\\ & \left[y_\sigma^{(i)}(t_k) - y_{pred}(t_k)\right]^T && (112)\end{aligned}$$

   (f) Calculate the Kalman Filter gain:

$$K(t_k) = P_{xy}P_y^{-1} \tag{113}$$

   (g) Calculate the innovation variable[5]:

$$e\,(t_k) = y(t_k) - y_{pred}(t_k) \tag{114}$$

   (h) *Calculate the state estimate (aposteriori estimate, or corrected estimate), which is used as the applied estimate, x_e:*

$$x_e(t_k) = x_{apost}\,(t_k) = x_{apri}\,(t_k) + K(t_k)e\,(t_k) \tag{115}$$

   (i) Estimate the covariance of aposteriori state estimate:

$$P_{apost}(t_k) = P_{apri}(t_k) - K(t_k)P_yK_k^T \tag{116}$$

The overall structure of the UKF can be represented by the block diagram shown in Figure 14 (which is the same block diagram as for the Extended Kalman Filter).

A.6 Augmentation of the state vector

If you want to estimate a parameter or an unknown component of a signal (variable) in addition to the basic state variables, you can augment the basic state vector with the appropriate number of state variables, and estimate these state variables together with the basic state variables in the normal way. These augmentation state variables are typically assumed to vary randomly but with a constant mean. For UKF

[5] Also denoted the innovation process.

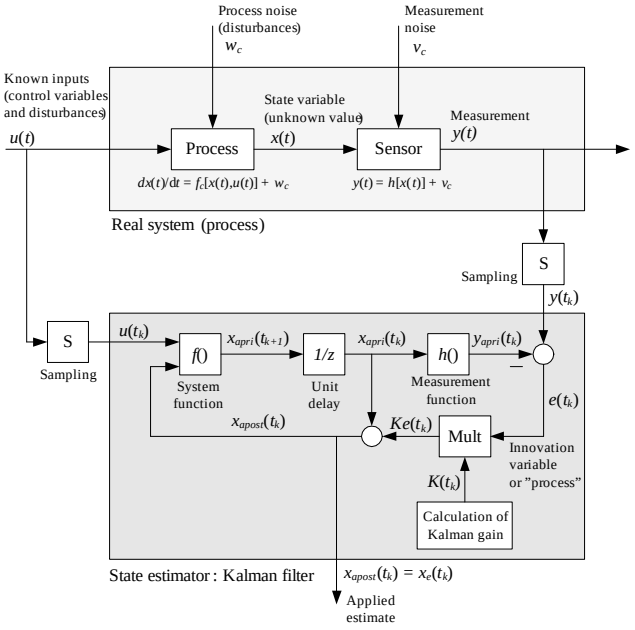

Figure 14: The Kalman filter

(as for EKF) the augmentation state variables are typically modelled as

$$\dot{x}_{aug}(t) = 0 + w_{aug} = w_{aug} \tag{117}$$

Once this state augmentation has been made, UKF is used as normally.

References

[1] Batstone, D. J., Keller, J., Angelidaki, I., Kalyuzhnyi, S. V., Pavlovstahis, S. G., Rozzi, A., Sanders, W. T. M., Siegrist, H., and Vavilin, V. A. (2002). *Anaerobic Digestion Model No. 1 (ADM1)*, Scientific and Technical Report No. 15, IWA Publising, London, UK.

[2] Bernard, O., Hadj-Sadok, Z., Dochain, D., Genovesi, A., Steyer, J.-P. (2001). *Dynamical Model Development and Parameter Identification for an Anaerobic Wastewater Treatment Process.* Biotechnology and Bioengineering, Vol. 75, No. 4.

[3] Boe K., Batstone D. J., Steyer J-P., Angelidaki I. (2010). *State indicators for monitoring the anaerobic digestion process*, Water Research 44, pp. 5773-5980.

[4] Dochain D. (2008.) Bioprocess Control, Wiley.

[5] Hill, D. T. (1983). *Simplified Monod kinetics of methane fermentation of animal wastes.* Agricultural Wastes, Vol. 5, pp. 1-16.

[6] Hill, D.T., Cobbs, S.A. and Bolte, J.P. (1987). *Using volatile fatty acid relationships to predict anaerobic digester failure.* Trans. ASAE, 30:496–501, 1987.

[7] Husain, A. (1998). *Mathematical models of the kinetics of anaerobic digestion - A selected review.* Biomass and Bioenergy Vol. 14, Nos. 5/6, pp. 561–571.

[8] Julier, S.J., Uhlmann, J.K. (1997). *A new extension of the Kalman Filter to nonlinear systems.* Int. Symp. Aerospace/Defense Sensing, Simul. and Controls, 3.

[9] Simon, D. (2006). *Optimal State Estimation.* John Wiley & Sons.

[10] Strømberg, S. (2010). *Development and Evaluation of Numerical Models for Anaerobic Digestion.* Master Thesis, Lund University, Sweden.

[11] Tchobanoglous, G., Burton, F. G., Stensel, H. D. (2003). *Wastewater Engineering: Treatment and Reuse.* Metcalf and Eddy, McGraw Hill Higher Education.